

Specialized robust CFD RANS microscale meteorological model for modelling atmospheric processes and transport of contaminants in urban and industrial areas

O.S. Sorokovikova <olga_sorokov@mail.ru>

D.V. Dzama <diman_sw@mail.ru>

D.G. Asfandiyarov <dasfandiyarov@ibrae.ac.ru>

The Nuclear Safety Institute of the Russian Academy of Sciences,
52, Bolshaya Tulkaya Street, Moscow, 115191, Russia

Abstract. State-of-the-art models of dispersion of contamination in the urban environment and industrial areas employ a CFD approach in order to calculate turbulent characteristics of flow around buildings with complex geometry. The main area of application of these models is to facilitate licensing of potentially hazardous facilities and assessment of meteorological conditions in the urban environment. The usage of the most popular commercial CFD software with regard to modelling flows in the urban environment is significantly limited by the requirement for computational mesh refinement near the surface of the building in order to adequately resolve the characteristic scales in the viscous and buffer sublayers. On the other hand, models based on the traditional gaussian approach cannot take into account the complex aerodynamic effects in order to calculate turbulent characteristics of flow around buildings with complex geometry, including the subtleties concerning atmospheric emissions of gas-aerosol substances. Therefore, the authors developed a robust, highly specialized CFD-RANS model and a calculation code for modelling the atmospheric dispersion of contamination under conditions of a complex three-dimensional geometry that do not require mesh refinement. The authors verified this model using extensive database obtained both in the course of field experiments as well as of wind tunnel experiments. The verification results showed that the developed model satisfies the acceptance criteria for the quality of modelling along with foreign general-purpose codes and highly specialized codes.

Keywords: microscale meteorological models; passive tracer transport; dose calculation.

DOI: 10.15514/ISPRAS-2018-30(5)-13

For citation: Sorokovikova O.S., Dzama D.V., Asfandiyarov D.G. Specialized robust CFD RANS microscale meteorological model for modelling atmospheric processes and contamination transport in urban and industrial areas. *Trudy ISP RAN/Proc. ISP RAS*, vol. 30, issue 5, 2018. pp. 213-234. DOI: 10.15514/ISPRAS-2018-30(5)-13

1. Introduction

A characteristic feature of the atmospheric transport of contaminants on a local scale is that the vertical and horizontal dimensions of the plume are comparable with the size of sharply outlined obstacles such as industrial buildings. Urban conditions entail three-dimensional flows around buildings. Hence, aerodynamic effects such as generation of recirculation zones, aerodynamic shadows, et cetera, dominate, thereby radically changing the local wind direction and velocity from the mean values at a larger scale. All these factors strongly influence the movement and dispersion of the contaminant plume. Figs. 1 and 2 show typical examples of the volume concentration distribution of contaminants near the surface obtained by three-dimensional modeling under urban conditions and under assumption of a smooth surface without obstacles with a uniform vertical profile of the wind velocity. A transition from red to blue signifies a difference in concentration of several orders of magnitude.

As can be seen from the figures, simplified approaches that do not take into account the real geometry of the obstacles lead to a non-realistic Gaussian distribution of contaminants.

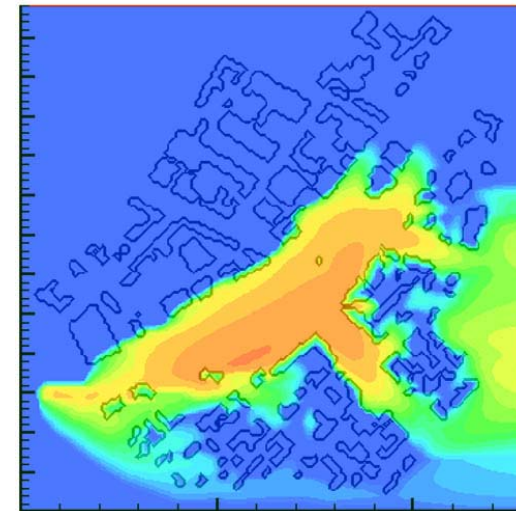


Fig. 1. Pollutant concentration distribution taking into account the 3D model of the urban area

State-of-the-art models of atmospheric dispersion of pollutants under urban conditions use the CFD approach to calculate the characteristics of the turbulent flow around buildings of arbitrary geometry. In accordance with the international classification, such models belong to the class of microscale meteorological models (MMM) [1]. The main area of application of such models is the analysis of the

environmental impact of industrial facilities, as well as the assessment of meteorological conditions in urban areas.

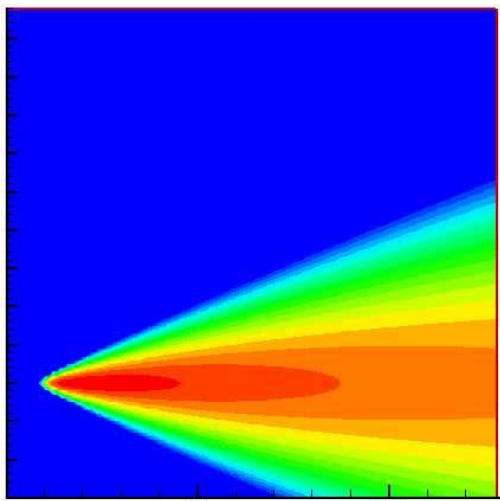


Fig. 2. Pollutant concentration distribution with a uniform wind field without buildings

A distinctive feature of the modern approach to modeling the transport of contaminants near industrial facilities and urban buildings is that it takes into account the three-dimensional pattern of flow around buildings. As a result, it has become possible to model aerodynamic effects and to obtain more realistic concentration distributions, which is fundamentally impossible within the framework of traditional Gaussian techniques.

Popular commercial CFD codes for pollutants atmospheric dispersion that take into account realistic geometry of urban or industrial buildings are mostly limited to simplified problems. The use of such codes for modeling flows around buildings with complex geometry is limited by the need to refine the computational mesh near the surfaces of buildings and the ground. Mesh refinement is necessary for the correct modelling of processes in the viscous and buffer layers. Though, such a significant mesh refinement can be very computationally demanding.

Current trends in tackling this problem are to employ highly specialized microscale meteorological models designed to simulate atmospheric processes taking into account 3D geometry of buildings.

A distinctive feature of highly specialized models is the parametrization of turbulent flow near the surfaces of the ground and buildings based on the Monin-Obukhov theory. Thus, one can avoid mesh refinement to resolve the viscous and buffer layers, thereby alleviating computational demands, in contrast with general-purpose software. A comparison was made with several foreign models of this class put to practical use.

This paper presents a model related to the MMM class. In comparison with other models of this class, its distinctive feature is the parametrization of the turbulent heat flux and the kinetic energy of turbulence near the surface under both stable and unstable temperature stratification.

In addition to calculating the concentration fields, the developed code calculates the doses of external and internal exposure (from inhalation). External exposure is divided into radiation from the cloud and the surface. Calculation of radiation from the cloud and the surface takes into account the shielding effect assuming that large buildings represented in a three-dimensional model of an industrial object completely absorb radiation.

Therefore, the developed model and the code allows modelling flows around buildings and calculation of volume and surface concentrations as well as the radiation situation in the territory of an industrial facility or a city. However, this paper describes only the MMM and verification of a part of the general software complex modelling key parameters of atmospheric non-isotropic processes (wind, turbulence). These parameters are the input data for modelling pollutants transport in case of complex geometry.

There is an analog put to practical use in Europe - a commercial software MISKAM (passive tracer, chemical compounds in urban areas, no version dealing with radioactivity issues) [2].

In the US, there is the FEM3MP model of the Livermore laboratory. It takes into account the specifics of radioactive contamination, but the model is not available to third-party users [3].

2. Model Description

The paper presents a CFD-RANS model belonging to the category of microscale meteorological models. This model allows obtaining fields of contaminant concentrations in the atmosphere, surface deposition of buildings and the ground as a result of the gas-aerosol release, taking into account the real geometry of the object, the stratification of the atmosphere, and heterogeneous turbulence in the atmospheric boundary layer.

The model is based on the incompressible Reynolds-averaged Navier-Stokes equations. Instead of using the wall functions in the first computational cell, the parametrization of heat flux and impulse is used in accordance with [4].

Input vertical profiles of speed and temperature are constructed in accordance with the model of the atmospheric boundary layer using the classification of the atmospheric stability classes according to Turner.

All calculated variables are treated as deviations from the hydrostatic balance. The Boussinesq approximation is used.

All physical quantities in the model are dimensional, the SI system is used.

The basic equations are as follows:

- Continuity equation

$$\operatorname{div} \bar{\mathbf{u}} = 0 \quad (1)$$

- Momentum transfer equation

$$\rho_0 \frac{\partial \bar{\mathbf{u}}}{\partial t} + \rho_0 (\bar{\mathbf{u}} \bar{\nabla}) \bar{\mathbf{u}} = -\bar{\nabla} \delta P + \bar{\nabla} (\rho_0 \nu_T \bar{\nabla}) \bar{\mathbf{u}} + \rho_0 \bar{\mathbf{g}} \frac{\delta \theta}{\theta_0} + \bar{\mathbf{f}} \quad (2)$$

- Heat transfer equation

$$\frac{d\theta}{dt} = \frac{\partial \theta}{\partial t} + \bar{\mathbf{u}} \bar{\nabla} \theta = \bar{\nabla} (\chi_T \bar{\nabla} \theta) \quad (3)$$

- The passive contaminant (i -th radionuclide) transfer equation

$$\frac{\partial C_i}{\partial t} + (\bar{\mathbf{u}} + \bar{\mathbf{w}}_i) \bar{\nabla} C_i = \bar{\nabla} (D_T \bar{\nabla} C_i) + Q_{C_i} \quad (4)$$

In (1) – (4), $\bar{\mathbf{u}}$ – three-dimensional vector of averaged flow velocity (m/s); ρ_0 – undisturbed input air density near the surface of the earth (constant, $\sim 1 \text{ kg/m}^3$); t – time (s); δP – pressure deviation from unperturbed hydrostatic at a given height with neutral stratification (Pa); ν_T – model coefficient of turbulent viscosity (m^2/s); $\bar{\mathbf{g}}$ – the vector of gravitational acceleration (m/s^2); θ_0 – unperturbed value of potential temperature at a given height (K); $\delta \theta$ – the deviation of the potential temperature from the unperturbed value at a given height (K); $\bar{\mathbf{f}}$ – possible force effect per unit volume of air (N/m^3); χ_T – model coefficient of turbulent thermal diffusivity associated with constant factor ν_T ; C_i – concentration value of the i -th component of the impurity (kg/m^3 or Bq/m^3 for radioactive impurity); $\bar{\mathbf{w}}_i$ – velocity vector of gravitational subsidence (for the aerosol component of the impurity, m/s); D_T – model coefficient of turbulent diffusion of the contaminants associated with constant factor ν_T (m^2/s); Q_{C_i} – dependent on the coordinate and time of the emission power of the i -th component (kg/s or Bq/s).

A two-layer model of turbulence is used for the closure of the basic equations.

The classical model of turbulence k – ε is applied to non-surface cells, that is, to those that do not have solid faces.

The kinetic energy equation for turbulence k is as follows:

$$\frac{\partial k}{\partial t} + \bar{\nabla} (k \bar{\mathbf{u}}) = \bar{\nabla} \left(\frac{\nu_T}{\sigma_k} \bar{\nabla} k \right) + S + G - \varepsilon, \quad (5)$$

where k is the kinetic energy of turbulence (m^2/s^2); σ_k – dimensionless empirical constant (equal to 1). The term G on the right-hand side of the equation is responsible for the generation of turbulent energy due to temperature stratification. The parameter G is proportional to the gradient of potential temperature:

$$\frac{\bar{\mathbf{g}}}{\theta} (\bar{\mathbf{u}}' \theta') = G = \frac{\nu_T}{\sigma_\theta} \bar{\nabla} \bar{\theta} \quad (6)$$

In (6), $\bar{\mathbf{u}}'$ and θ' – pulsations of the vector of the flow velocity and potential temperature, respectively; σ_θ – dimensionless empirical constant (0.9).

The first term on the right-hand side of the equation (5) is a parameterization of the transfer of turbulent energy by velocity pulsations:

$$-\frac{\partial \overline{u'_j k'}}{\partial x_j} = \frac{\partial}{\partial x_j} \left(\frac{\nu_T}{\sigma_k} \frac{\partial k}{\partial x_j} \right) \quad (7)$$

The parameter S on the right side of the equation (5) is responsible for the generation of turbulence energy due to shear deformations and is determined as follows (summation is performed over repeated indices in accordance with the Einstein rule):

$$S = \nu_T \left[\frac{\partial u_i}{\partial x_j} + \frac{\partial u_j}{\partial x_i} \right] \frac{\partial u_i}{\partial x_j} \quad (8)$$

In the definition (8), u_i is the i -th component of the averaged flow velocity. The transfer equation for turbulent energy dissipation is as follows:

$$\frac{\partial \varepsilon}{\partial t} + \bar{\nabla} (\varepsilon \bar{\mathbf{u}}) = \bar{\nabla} \left(\frac{\mu_T}{\sigma_\varepsilon} \bar{\nabla} \varepsilon \right) + \frac{\varepsilon}{k} (C_{\varepsilon 1} S + C_{\varepsilon 3} G) S - C_{\varepsilon 2} \frac{\varepsilon^2}{k} \quad (9)$$

In the equation (9), ε – the turbulent energy dissipation rate (m^2/s^3); σ_ε , $C_{\varepsilon 1}$, $C_{\varepsilon 2}$, and $C_{\varepsilon 3}$ are dimensionless empirical constants, which are equal to, respectively: 1.3; 1.21; 1.92; 1.44 (for atmospheric problems).

The transfer equations (5) and (9) have five empirical constants: $C_{\varepsilon 1}$, $C_{\varepsilon 2}$, $C_{\varepsilon 3}$, σ_k , σ_ε . In this form, model equations k – ε are widely used to simulate turbulence, as, for example, in [5].

The coefficient of turbulent viscosity, which is used in the Reynolds-averaged Navier-Stokes equations, is calculated using the following formula:

$$\nu_T = C_\mu \frac{k^2}{\varepsilon} \quad (10)$$

In (10), C_μ is a dimensionless empirical constant (0.03 – for atmospheric problems).

In contrast with the classical k – ε turbulence model, the following parametrization for k and ε is used in the subsurface cells. These values are determined by the value of the dynamic velocity (friction velocity), which is determined by the value of the tangential component of the velocity along a solid surface and also depends on the stability class of the atmosphere. For example, the following relation is used for unstable (A, B, C according to Turner's classification with minor modifications) and neutral stratification (D according to the same classification) [4]:

$$u(z) = \frac{u^*}{\kappa} \left[\ln\left(\frac{z}{r}\right) - \left\{ \ln\left(\frac{1+\xi^2}{2}\right) + 2 \ln\left(\frac{1+\xi}{2}\right) - 2 \arctg(\xi) + \frac{\pi}{2} \right\} \right], \quad (11)$$

where:

- z – the distance from the measurement point of the tangential component of the flow velocity to the streamlined surface (m);
- $u(z)$ – the tangential component of the averaged flow velocity (m/s);
- u^* – the actual value of the dynamic velocity or friction velocity (m/s);
- $\kappa=0.41$ – the Karman constant;
- r – the surface roughness, m;
- γ – a dimensionless constant, equal to 15;
- L – the Monin-Obukhov scale, which depends on the stability class of the atmosphere [6] (the values are given in Table 1);
- $\xi = (1 - \gamma z / L)^{1/4}$, dimensionless parameter.

Table 1. Monin-Obukhov scale depending on the stability class

Atmosphere stability class	A	B	C	D	E	F	G
Mean value	-5	-25	-70	-500	55	5	1
Minimum value	-10	-40	-100	$-\infty$	10	1	0
Maximum value	0	-10	-40	± 100	100	10	1

To determine the turbulent heat flux $\overline{w'\theta'}$, where w' – the pulsation of the vertical component of the flow velocity (m/s), and θ' – the potential temperature pulsation (K), (12) and (13) parameterizations are used, which are given below [7]. In the case of unstable and neutral stratification, these parameterizations are as follows:

$$\overline{w'\theta'} = -u^* \frac{\theta^{AIR} - \theta^{GROUND}}{\frac{R}{\kappa} \left(\ln\left(\frac{z}{r}\right) - 2 \ln\left(\frac{1+\eta^2}{2}\right) \right)} \quad (12)$$

For stable stratification:

$$\overline{w'\theta'} = -u^* \frac{\theta^{AIR} - \theta^{GROUND}}{\frac{R}{\kappa} \left(\ln\left(\frac{z}{r}\right) + \frac{\beta z}{RL} \right)} \quad (13)$$

where $\eta = (1 - \lambda z / L)^{1/4}$, $R=0.74$, $\lambda=9$; $\beta=4.7$ (all are dimensionless constants); θ^{AIR} – the potential temperature in the surface layer; θ^{GROUND} – the potential temperature of the earth, which is kept constant during calculations.

The use of such parametrizations limits the size of the computational mesh to be 20–30 times larger than the roughness value.

To calculate k and ε , (14) and (15) formulas are used in the near-surface cells, accordingly:

$$k = \frac{u_*^2}{C_\mu^{1/2}}, \quad (14)$$

$$\varepsilon = \frac{u_*^3}{\kappa z}. \quad (15)$$

The model requires the following input data: three-dimensional Cartesian grid; three-dimensional models of the buildings; wind speed and direction at a height of 10 m; atmospheric stability class; geographical latitude of the object; roughness value of the underlying surface. The initial and boundary conditions for the hydrothermodynamic problem are set automatically from the data listed above, which is provided by the user.

To solve the transfer problem, it is necessary to set the parameters of the source of release: the release rate, the nuclide composition of the source, the position of the source in space. For each nuclide, the dry precipitation rate is required. If necessary, there may be several point sources, and they can be placed at different points in the computational domain.

3. Verification and Validation

Below there are some results of verification of the model and examples of its application.

Studies have shown that the existing data sets obtained during the experiments are not always suitable for the verification of microscale models. This impelled the international scientific community to initiate the creation of a database that would be more suitable for these purposes [8].

There are two approaches to solve this problem. The first approach is to create a database for verification by collecting information from experiments conducted in wind tunnels. The second approach gives priority to experiments conducted under natural atmospheric conditions [9].

Both approaches have their pros and cons, it is very difficult to simulate some phenomena in a wind tunnel experiment, such as: stratification, thermal effects as a result of heating or cooling of building surfaces, chemical reactions, and aerosol precipitation.

On the contrary, a coarse measurement grid, which is typical of field experiments, does not allow accurate estimation of the parameters of the inhomogeneous and unsteady flow, which is necessary for comparison with the data obtained by modeling.

At the present time, there exist quantitative parameters of the quality of simulation results obtained by using microscale meteorological models. In the literature, the simulation results are mainly characterized by two quantitative parameters.

Quantitative assessment of simulations is based on the comparison of two series of the same size consisting of C_{calc} and C_{obs} – model (calculated) and measured values for a given physical quantity, respectively. Each element of these two series corresponds to a certain point of measurement of the physical quantity value, which can be either one of the components of the flow velocity or tracer concentration.

In order to verify the model, the quality of modeling was estimated by the following values [1]:

- FA-2 (factor of 2 of observation) shows the proportion of the total number of measurement points for which the condition (17) is met:

$$FA-2 = \frac{N}{n} = \frac{\sum_{i=1}^n N_i}{n}, \quad (16)$$

$$N_i = \begin{cases} 1, & \text{if } 1/2 \leq C_{calc}^i / C_{obs}^i \leq 2 \\ 1, & \text{if } C_{obs}^i \leq W \\ 0, & \text{else} \end{cases} \quad (17)$$

- Hit Rate is defined as:

$$HR = \frac{N}{n} = \frac{1}{n} \sum_{i=1}^n N_i, \quad (18)$$

$$N_i = \begin{cases} 1, & \text{if } \left| \frac{C_{calc}^i - C_{obs}^i}{C_{obs}^i} \right| \leq D \\ 1, & \text{if } \left| C_{calc}^i - C_{obs}^i \right| \leq W \\ 0, & \text{else} \end{cases} \quad (19)$$

In (17) and (19), C_{calc}^i and C_{obs}^i – elements of the series of the calculated and measured physical quantities with the same index. In (16), N – the total number of pairs (measurement points) for which the condition (17) is fulfilled, n – dimensions of the input arrays (measured and calculated), that is, the total number of measurement points. In (17), W – the threshold value of the measured flow velocity or concentration, below which the condition (17) is considered to be satisfied regardless of the value of the calculated flow velocity or concentration.

Similarly, in the ratio (18), N – the total number of pairs for which the condition (19) is fulfilled; D – the accepted relative error of calculation of a physical quantity; W – the threshold value of the absolute error of calculation of the physical parameter, below which the condition (19) is considered to be satisfied regardless of the actual measured and calculated values.

The parameter D takes into account the relative uncertainty of the comparison, and the parameter W reflects the measurement uncertainty in the experiment. The value of D recommended by the expert community is 25% [5, 10]. The value of W is determined using statistical analysis of the variation of measurements in a series of experiments conducted under the same conditions.

Within the COST732 project [10], a database called CEDVAL [1] (compilation of experimental data for the validation of microscale meteorological models) was created, consisting of a set of experiments in a wind tunnel. The geometry of the obstacles was of varying difficulty: from one obstacle in the form of a rectangular parallelepiped to experiments in which there were four obstacles with slanted roofs, as well as experiments with an almost regular arrangement of 21 a rectangular parallelepipeds.

Let us focus on the experiments themselves. Verification was performed for a series of experiments A and B.

Experiments of the A1-1 series were characterized by a frontal flow around one obstacle in the form of a rectangular parallelepiped, the dimensions of which are 20 m × 30 m × 50 m. In this series of experiments, pairs of flow velocity components in (u, w) and (u, v) were measured in two mutually perpendicular planes.

In experiments of series A1-2 and A1-3, a rectangular parallelepiped strongly elongated along the Y-axis, the dimensions of which are 25 m × 324 m × 25 m, appeared as an obstacle. Wind direction is along the X-axis. In experiments A1-2, measurements were taken in the vertical plane running through the center of the obstacle. The pair of components of the flow velocity (u, w) were measured. In experiments A1-3, measurements were carried out both in the horizontal and in the vertical plane. In the horizontal plane, the components (u, v) were measured, and the vertical components (u, w).

In a series of experiments A1-4, a cube measuring 25 m was frontally flown around. The measurements of the components of the flow velocity were carried out in several horizontal and vertical sections. In horizontal sections, pairs of components (u, v) were measured, in vertical sections – pairs (u, w).

In experiments of the A1-5 series, a rectangular parallelepiped measuring 20 m × 30 m × 25 m was frontally flown around. A constant point source of the tracer acted near the obstacle. In the experiments, the steady-state values of the tracer concentration in several planes of different orientations were measured.

In experiments of the A1-6 series, a cube measuring 25 meters flowed around one of the faces at an angle of 45°. In this series of experiments, pairs of flow velocity

components (u, v) and (u, w) were measured in the horizontal and vertical planes, respectively.

In the experiments of A1-7 series, a cubic obstacle was also considered, but the flow was made at an angle of 40°. In this series of experiments, several components of the flow velocity were measured in several planes of different orientations.

In the experiments of B1-1 series, there were 20 obstacles measuring 20 m × 30 m × 25 m each, arranged in a 7 × 3 pattern (one building of 21 points was missing). Measurements of a pair of velocities (u, v) were carried out in one horizontal plane, a pair (u, w) – in four vertical planes. In addition, a constant point source of the tracer was present in the experiments and the steady-state field of its concentration in one plane was measured.

In the experiments of B1-2 series, there were 4 ring obstacles with dimensions of 250 m × 250 m × 60 m, arranged according to a 2 × 2 scheme. An annular obstacle could be obtained geometrically by separating a smaller parallelepiped from a rectangular parallelepiped with dimensions of 130 m × 130 m × 60 m. The pairs of velocity components (u, v) and (u, w) were measured in two horizontal and two vertical planes.

In the experiments of B1-3 series, 4 obstacles were distant along the X-axis to a greater distance than in the experiments of B1-2 series. The pairs of components (u, w) and (u, v) were measured in the vertical and horizontal planes.

In the experiments of B1-4, B1-5, and B1-6 series, there were similar ring obstacles, but with a more complex roof shape, part of which had a sloping shape. The wind direction in these experiments differed. In all experiments, pairs of components of the flow velocity (u, w) and (u, v) were measured in several planes of different orientations.

The verification results based on the CEDVAL database include about 20,000 single measurements and are presented in Table 2. This table presents the parameters FA-2 and Hit Rate for the three components of the flow velocity.

The average value of FA-2 and Hit Rate is defined as the weighted sum of these characteristics over all experiments. The weight in each experiment is equal to the ratio of the number of data points in this experiment to the total number of measurement points in all experiments.

Table 2. The total values of the statistical parameters FA-2 and HIT RATE for the three components of the flow velocity for all experiments (series A and B)

Criterion	Value
FA-2 (U)	87%
FA-2 (V)	96%
FA-2 (W)	93%
Hit-rate (U)	76%

Hit-rate (V)	82%
Hit-rate (W)	75%

In Table 2, U, V, and W are the components of the flow velocity along the X, Y, and Z axes, respectively. The verification results in Table 2 are given for all experiments of A and B series. These results were obtained by combining the data sets in all experiments. For several series of experiments, the verification results are given below.

In accordance with the COST732 project documents, the acceptance criterion for microscale meteorological models is 66% and 55% for FA-2 and Hit Rate, respectively.

Methods for analyzing the results of modeling against measurement data have been fairly well developed and are widely used in practice in relation to microscale meteorological models. For verification other quantitative characteristics are also used.

PCC (Pearson correlation coefficient):

$$P = \frac{\sum_{i=1}^n (C_{calc}^i - \bar{C}_{calc})(C_{obs}^i - \bar{C}_{obs})}{\sqrt{\sum_{i=1}^n (C_{calc}^i - \bar{C}_{calc})^2 \sum_{i=1}^n (C_{obs}^i - \bar{C}_{obs})^2}}, \quad (20)$$

where P is in the range from -1 to 1 . The ideal case for the model is achieved at $P = 1$. In the ratio (20), \bar{C}_{calc} and \bar{C}_{obs} are the average values of the calculated and measured physical quantity over the whole array. Each of the three summations is performed over all pairs of arrays of measured and calculated values.

Statistical parameters formulated in terms of overestimation or underestimation of measured values and representing the average offset of the calculated values are also widely used. The following criteria are the most popular in this category.

BIAS estimates the deviation of the calculated average values from the measured, expressing the deviation in physical units of measurement (in this case, in units of concentration):

$$BIAS = \bar{C}_{calc} - \bar{C}_{obs} = \frac{1}{N} \sum_{i=1}^N (C_{calc}^i - C_{obs}^i) \quad (21)$$

The BIAS value shows the absolute value of underestimating or overestimating the calculated values in comparison with the measured ones.

SAA (Scaled Average Angle difference) is a weighted average angular deviation, which is used less frequently [11], but was used to verify the developed model:

$$SAA = \frac{\sum_{i=1}^N |U_i| |\varphi_i|}{\sum_{i=1}^N |U_i|} \quad (22)$$

where φ_i – the angle between the calculated and measured flow velocity, $|U_i|$ – the module of the measured flow velocity at the i -th point.

SAA is used if there is a detailed measurement network that can contain data on the direction and magnitude of the wind in several sections. It characterizes the accuracy of wind direction modeling by calculating a weighted sum with weights equal to the modulus of the flow velocity. The greater the flow velocity at a given point, the more it contributes to the total amount.

The results of the statistical comparison of calculated and measured values for the A1 experiment are shown below (in Tables 3-5).

Table 3. Statistical criteria for the longitudinal velocity component (along the main flow). Vertical section. Experiment A1

Criterion	Value	Best value
FA-2	98%	100%
HR	90%	100%
BIAS	-0.09260	0
PCC	0.96194	1
SAA	6.85260	0

Table 4. Statistical criteria for the vertical velocity component. Vertical section. Experiment A1

Criterion	Value	Best value
FA-2	98%	100%
HR	90%	100%
BIAS	-0.09260	0
PCC	0.96194	1
SAA	6.85260	0

Table 5. Statistical criteria for the longitudinal velocity component (along the main flow). Horizontal section. Experiment A1

Criterion	Value	Best value
FA-2	93%	100%

HR	75%	100%
BIAS	-0.46255	0
PCC	0.93649	1
SAA	7.61284	0

In addition to laboratory experiments, the comparison of simulated and measured concentration values was carried out using the data of the experiment JOINT URBAN 2003 (downtown Oklahoma). The essence of the experiments consisted in the artificial creation of a permanent source of atmospheric emission of a passive tracer for the subsequent restoration of the pollution pattern under the conditions of the complex urban development of the center of Oklahoma. Elegas (SF_6) was used as a passive tracer that does not enter into chemical reactions and does not precipitate on solid surfaces. In one of the experiments, the results of which were used to compare the results of the described model, SF_6 gas was ejected at a constant intensity for half an hour with neutral temperature stratification. During the same period of time, the concentration of SF_6 gas in the air was continuously monitored with high-precision equipment, both using stationary and mobile laboratories (installed on vehicles). The steady-state concentrations of SF_6 -gas obtained by the described model with the highest readings of high-precision sensors were compared. In the same period of time, the flow was measured at various altitudes with the help of high-precision equipment. This dataset allowed finding an approximation of the vertical input profile of the horizontal component of the wind speed, which was used to simulate hydrodynamics using the developed model.

Fig. 3 shows the position of the source against the background of the three-dimensional model of the city. Fig. 4 shows the concentration isosurfaces. Fig. 5 shows the position of the source against the background of the map and the positions of the concentration measurement points. Fig. 6 shows profiles of measured and calculated tracer concentrations depending on the number of the measurement point. Green squares represent the calculation results for the developed model, blue triangles – measurement data by stationary stations.

The tracer concentration field on the streets of a real city can be very complex. The ratio of concentrations at close points can be at the level of three orders of magnitude. A significant discrepancy was obtained at station number 13, where the model results are underestimated compared to the measurement results. However, the absolute maximum concentration (measurement station 20) corresponds to the model results with a relative accuracy of 5%.

Let us consider the situation associated with the measuring station 13, where there was the greatest discrepancy. Fig. 7 shows the location of this station (and station 14), as well as the isolines of the calculated tracer concentration in this area. It can be noted that the concentration field of the tracer in this area is highly non-uniform – the horizontal gradient is high. Consequently, the concentration of the tracer in the vicinity of point 13 is much greater than in the point itself.

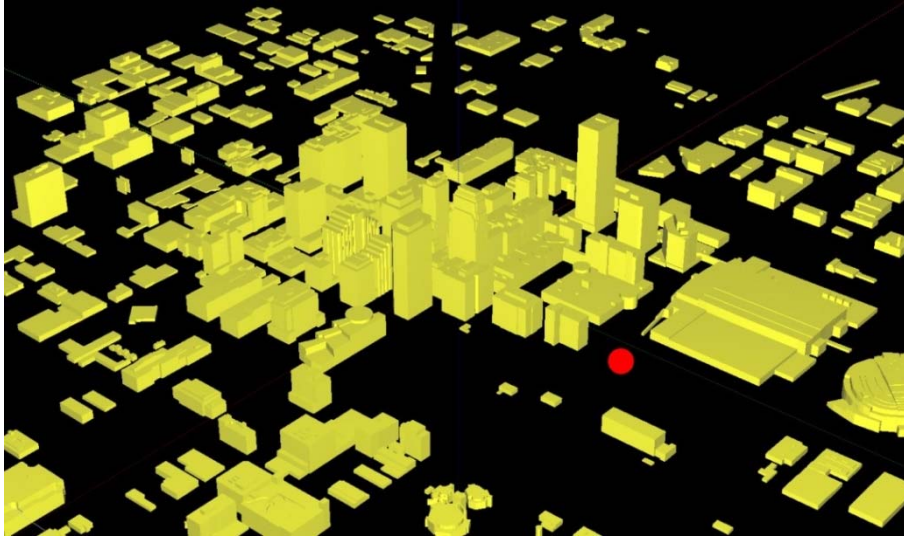


Fig. 3. 3D model of the center of Oklahoma city

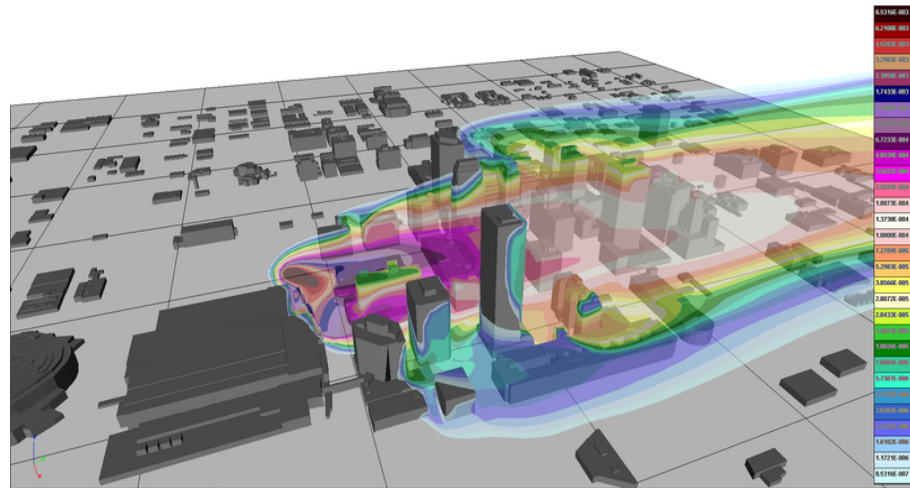


Fig. 4. Isosurfaces of concentration (results of modeling)



Fig. 5. Release point and measurement stations

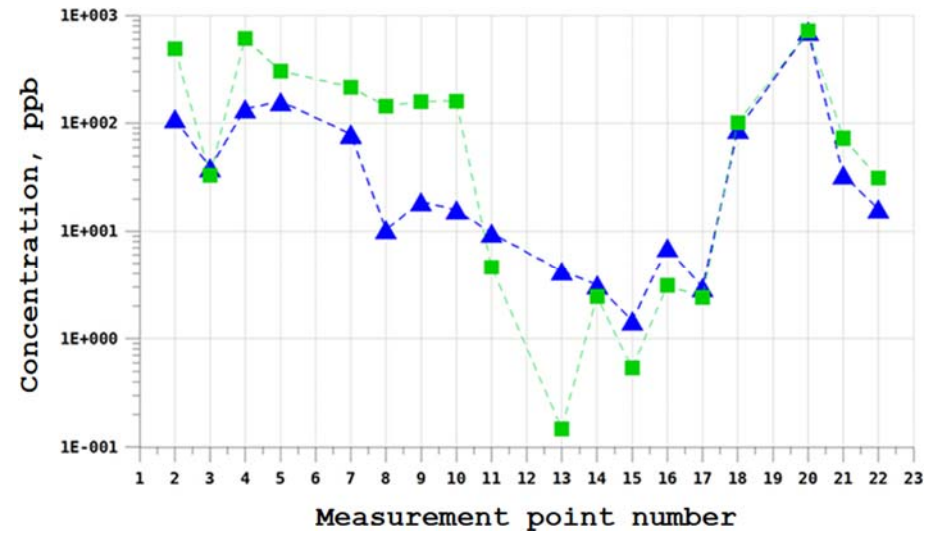


Fig. 6. Model results against experimental values

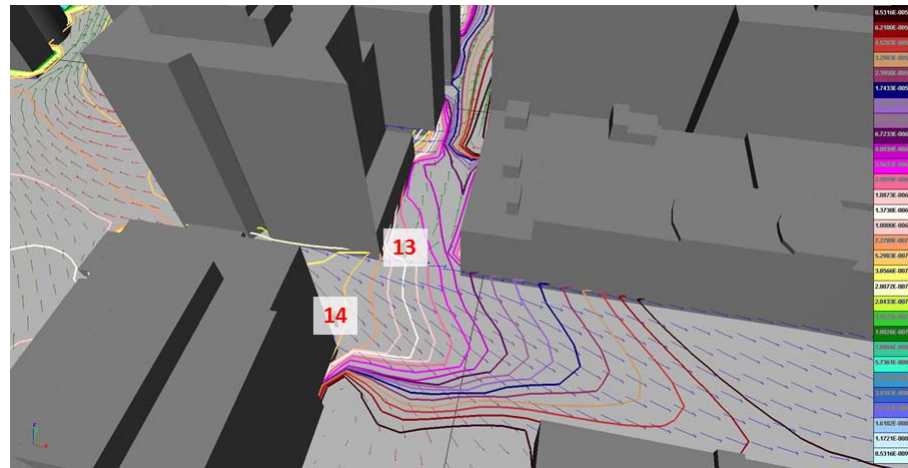


Fig. 7. Isolines of surface concentration in the vicinity of station 13 and 14

In addition to the calculations of the concentration fields in the model, the doses of external and internal exposure (from inhalation) are calculated. External exposure is divided into radiation from the cloud and the contaminated surface. Calculation of doses from external exposure is made taking into account the effect of radiation shielding by buildings, on the basis of the assumption that large buildings represented in a three-dimensional model of an industrial object completely absorb the dose-forming radiation.

The results of simulation at the Beloyarsk NPP is shown in Fig. 8 as an example of practical usage of the model. A hypothetical scenario characterized by loss of systemic and reliable power supply (failure of active reactor shutdown systems, failure of the EHRS (emergency heat removal system)), depressurization of 25% of nuclear reactor core fuel elements, which have a maximum burnout was considered. One of the nuclides of the release is ^{137}Cs ($5 \cdot 10^{13}$ Bq). The duration of the release was 30 minutes and the source was located at the level of the roof of the reactor building (in Fig. 8 – building with a pipe). Fig. 8 shows distribution of ^{137}Cs surface contamination of land and buildings (Bq/m^2) at the time of the end of the source action.

4. Cross-verification of the developed code with foreign calculation codes

The results of the cross-verification based on the Hit Rate statistical parameter for the vertical component of the flow velocity of the developed model with different models are shown in Fig. 9. The measurement data was obtained as a result of a tunnel experiment conducted by the University of Hamburg in the framework of the COST732 project.

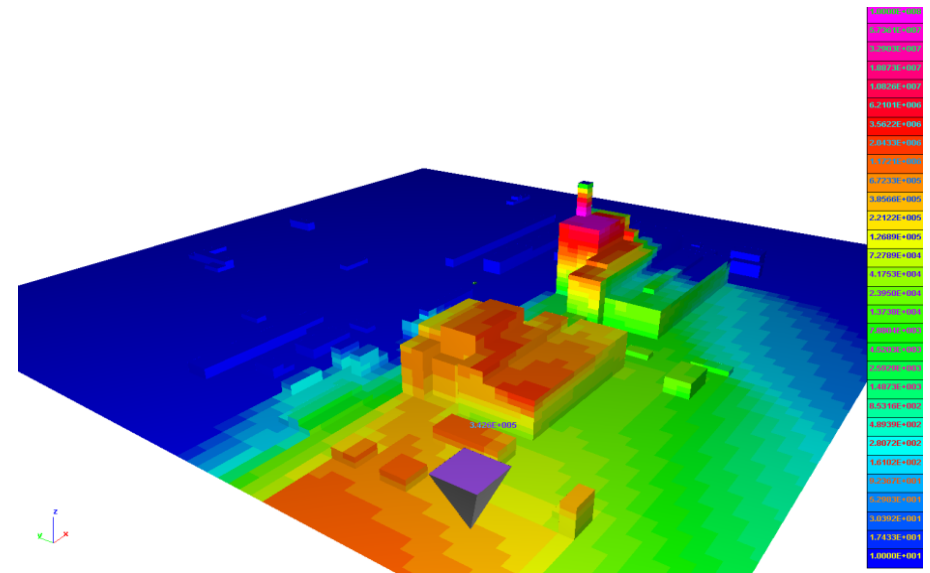


Fig. 8. Visualization of a concentration deposition field in the area of the Beloyarsk NPP.

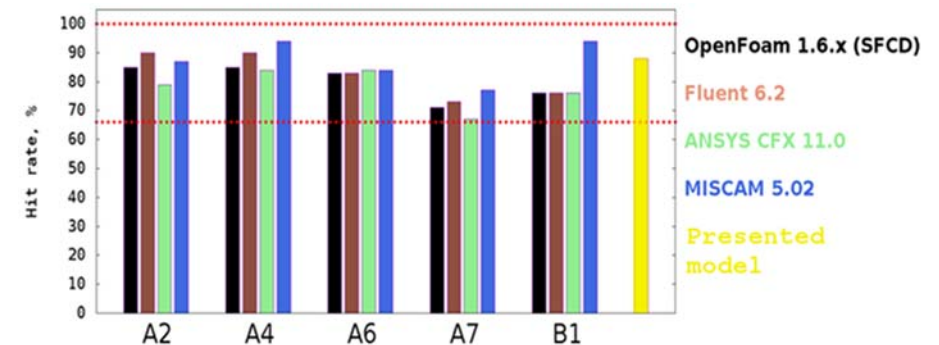


Fig. 9. Results of cross-verification of the developed model

Cross-verification was carried out using the results of modeling of five different experiments (A2, A4, A6, A7, B1 of the COST 732 database – Fig. 9) by four different calculation codes. Each component of the flow velocity was compared. Fig. 9 shows the results of verification of the longitudinal (along the X-axis — typical wind direction in all experiments) components of the flow velocity. The Hit Rate values gained by foreign models are presented for several experiments of series A and one experiment of series B separately. For the model described in this paper, the Hit Rate value is given in sum for all the experiments carried out, both series A and series B.

Thus, the verification of the model on an international database showed that the calculation code and the model meet the criterion of the modeling quality developed by the international expert community [9].

5. Conclusion

In accordance with current trends in applied computational meteorology, a reliable CFD model has been developed. The verification matrix of the developed model and design code contains various data obtained from both large-scale field experiments in a real city (Oklahoma City) and from laboratory experiments. It is shown that the developed model meets the quality criteria of the simulation, defined by the expert community for models of the same class.

References

- [1]. Michael Schatzmann, Helge Olesen, Jörg Franke: COST 732 Model Evaluation Case Studies: Approach and Results. University of Hamburg Meteorological Institute Centre for Marine and Atmospheric Sciences, 2010, <http://www.mi.uni-hamburg.de/Official-Documents.5849.0.html>
- [2]. SoundPlan. MISKAM advanced. <http://www.soundplan.eu/english/soundplan-air-pollution/miskam-advanced/>
- [3]. Stevens T. Chan, Martin J. Leach. A Validation of FEM3MP with Joint Urban 2003 Data. Journal of applied meteorology and climatology. Vol. 46. 2007. pp. 2127-2146 Data base CEDVAL at Hamburg University, <http://www.mi.zmaw.de/index.php?id=432>
- [4]. Randerson D., Atmospheric science and Power production. Technical Information Center, Office of Scientific and Technical Information. United States Department of Energy. – Vol. 1. – [S.1.], 1994 INTERNATIONAL ATOMIC ENERGY AGENCY, Isotope Techniques in Water Resources Development and Management, C&S Papers Series No. 2/C, IAEA, Vienna (1999) (CD-ROM).
- [5]. VDI (2005). Environmental meteorology – Prognostic microscale windfield models – Evaluation for flow around buildings and obstacles. VDI guideline 3783, Part 9. BeuthVerlag, Berlin.
- [6]. V.V. Belikov, V.M. Goloviznin, U.V. Katishkov et. all Proceeding of IBRAE RAS/ Ed. By L.A. Bolshov Issue 9 Modeling of radionuclide transport in the environment. Moscow:-Nauka, 2007.-229pp.
- [7]. Deardorff D.W., Parameterization of the planetary boundary layer for use in general circulation models, Mon. Wea. Rev., Vol. 100, №2, 1972.
- [8]. COST ES1006 – Best practice guidelines, COST action ES1006, april 2015. ISBN: 987-3-9817334-0-2
- [9]. Special Issue Joint Urban 2003. Journal of Applied Meteorology and Climatology, Volume 46, Issue 12 (December 2007)
- [10]. Jörg Franke, Antti Hellsten, Heinke Schlünzen and Bertrand Carissimo: Best practice guideline for the CFD simulation of flows in the urban environment. COST 732 report, Hamburg, 2007, ISBN: 3-00-018312-4
- [11]. A Validation of FEM3MP with Joint Urban 2003 Data Stevens T. Chan and Martin J. Leach Lawrence Livermore National Laboratory, Livermore, California 94551, USA

Специализированная робастная CFD RANS микромасштабная метеорологическая модель для моделирования атмосферных процессов и переноса примеси в условиях городской и промышленной застройки

О.С. Сороковикова <olga_sorokov@mail.ru>

Д.В. Дзама <diman_sw@mail.ru>

Д.Г. Асфандияров <dasfandiyarov@ibrae.ac.ru>

Институт проблем безопасного развития атомной энергетики РАН,
115191, Россия, г. Москва, ул. Большая Тульская, д. 52

Аннотация. В последние годы в мировой практике существует тенденция к использованию специализированных CFD моделей в задачах вычислительной метеорологии. К таким задачам относится, в частности, задача обоснования безопасности промышленных объектов, в том числе радиационно-опасных. Эта тенденция обусловлена тем фактом, что применение универсальных инженерных кодов общего назначения требует изрядных вычислительных мощностей и связано это в первую очередь с необходимостью сгущения расчётной сетки к поверхностям земли и зданий для разрешения вязкого и промежуточного слоёв. С другой стороны, гауссовы модели не могут учесть сложные аэродинамические эффекты, возникающие при обтекании зданий сложной конфигурации, в том числе описать все тонкости обтекания сооружений примесью при атмосферных выбросах газо-аэрозольных веществ. Поэтому авторами была разработана робастная узкоспециализированная CFD-RANS модель и расчётный код для моделирования атмосферной дисперсии примеси в условиях сложной трёхмерной геометрии, не требующие сгущения сеток. Авторы работы провели верификацию этой модели на различных данных, полученных как в ходе натурных крупномасштабных, так и в ходе лабораторных туннельных экспериментов. Для этих целей была использована, в частности, рекомендованная международным экспертным сообществом база данных и соответствующие статистические характеристики соответствия рассчитанных и полученных в ходе экспериментов значения компонент скорости течения и концентрации примеси. Результаты верификации показали, что разработанная модель удовлетворяет приёмочным критериям качества моделирования наравне с зарубежными кодами общего назначения и узкоспециализированными кодами.

Ключевые слова: микромасштабные метеорологические модели; перенос примеси; расчет доз.

DOI: 10.15514/ISPRAS-2018-30(5)-13

Для цитирования: Сороковикова О.С., Дзама Д.В., Асфандияров Д.Г. Специализированная робастная CFD RANS микромасштабная метеорологическая модель для моделирования атмосферных процессов и переноса примеси в условиях городской и промышленной застройки. *Труды ИСП РАН*, том 30, вып. 5, 2018 г., стр. 213-234 (на английском языке). DOI: 10.15514/ISPRAS-2018-30(5)-13

Список литературы

- [1]. Michael Schatzmann, Helge Olesen, Jörg Franke: COST 732 Model Evaluation Case Studies: Approach and Results. University of Hamburg Meteorological Institute Centre for Marine and Atmospheric Sciences, 2010, <http://www.mi.uni-hamburg.de/Official-Documents.5849.0.html>
- [2]. SoundPlan. MISKAM advanced. <http://www.soundplan.eu/english/soundplan-air-pollution/miskam-advanced/>
- [3]. Stevens T. Chan, Martin J. Leach. A Validation of FEM3MP with Joint Urban 2003 Data. *Journal of applied meteorology and climatology*. Vol. 46. 2007. pp. 2127-2146 Data base CEDVAL at Hamburg University, <http://www.mi.zmaw.de/index.php?id=432>
- [4]. Randerson D., Atmospheric science and Power production. Technical Information Center, Office of Scientific and Technical Information. United States Department of Energy. – Vol. 1. – [S.1.], 1994 INTERNATIONAL ATOMIC ENERGY AGENCY, Isotope Techniques in Water Resources Development and Management, C&S Papers Series No. 2/C, IAEA, Vienna (1999) (CD-ROM).
- [5]. VDI (2005). Environmental meteorology – Prognostic microscale windfield models – Evaluation for flow around buildings and obstacles. VDI guideline 3783, Part 9. BeuthVerlag, Berlin.
- [6]. V.V. Belikov, V.M. Goloviznin, U.V. Katishkov et. all Proceeding of IBRAE RAS/ Ed. By L.A. Bolshov Issue 9 Modeling of radionuclide transport in the environment. Moscow:-Nauka, 2007.-229pp.
- [7]. Deardorff D.W., Parameterization of the planetary boundary layer for use in general circulation models, *Mon. Wea. Rev.*, Vol. 100, №2, 1972.
- [8]. COST ES1006 – Best practice guidelines, COST action ES1006, april 2015. ISBN: 987-3-9817334-0-2
- [9]. Special Issue Joint Urban 2003. *Journal of Applied Meteorology and Climatology*, Volume 46, Issue 12 (December 2007)
- [10]. Jörg Franke, Antti Hellsten, Heinke Schlünzen and Bertrand Carissimo: Best practice guideline for the CFD simulation of flows in the urban environment. COST 732 report, Hamburg, 2007, ISBN: 3-00-018312-4
- [11]. A Validation of FEM3MP with Joint Urban 2003 Data Stevens T. Chan and Martin J. Leach Lawrence Livermore National Laboratory, Livermore, California 94551, USA